XRM Readout Design Review

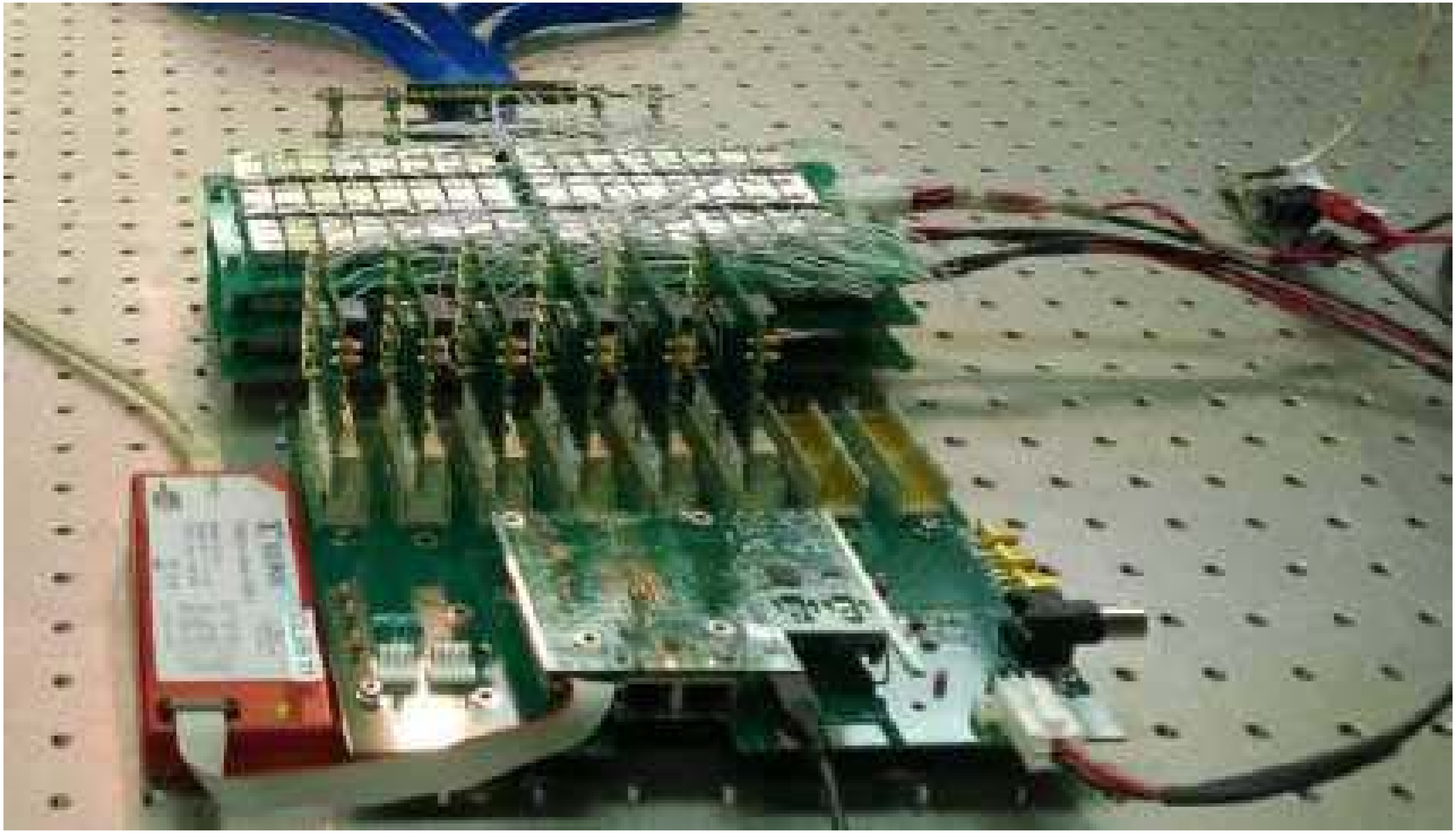

G. Varner

August 27, 2015

SuperKEKB and BelleII

- Major upgrade of accelerator and detector for searches for physics “beyond the standard model”

- KEKB luminosity NOT limited by ability to squeeze beams, but by beam-beam interactions

- Real-time beam diagnostics are vital:
  - **Nanometer size beams drives x-ray monitoring**
  - Infrared and optical synchrotron light not able to resolve true bunch size
  - Use technique developed for x-ray astronomy
  - Flexible operating modes [4x BX all the time, through full orbit logging (at ~200 Hz)]

KEKB to SuperKEKB

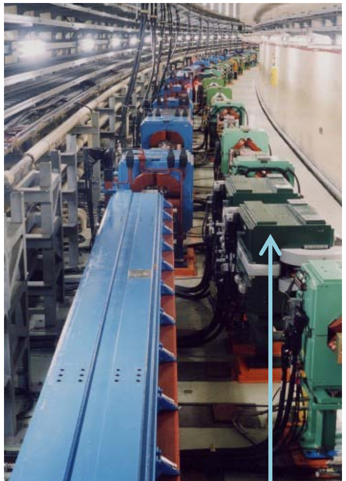

Replace short dipoles with longer ones (LER)

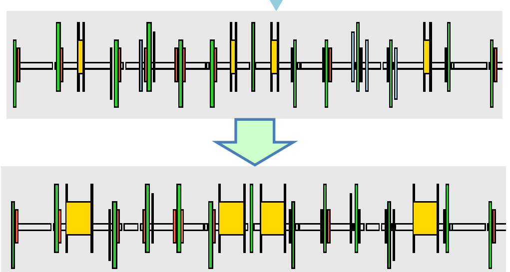

Redesign the lattices of HER & LER to squeeze the emittance

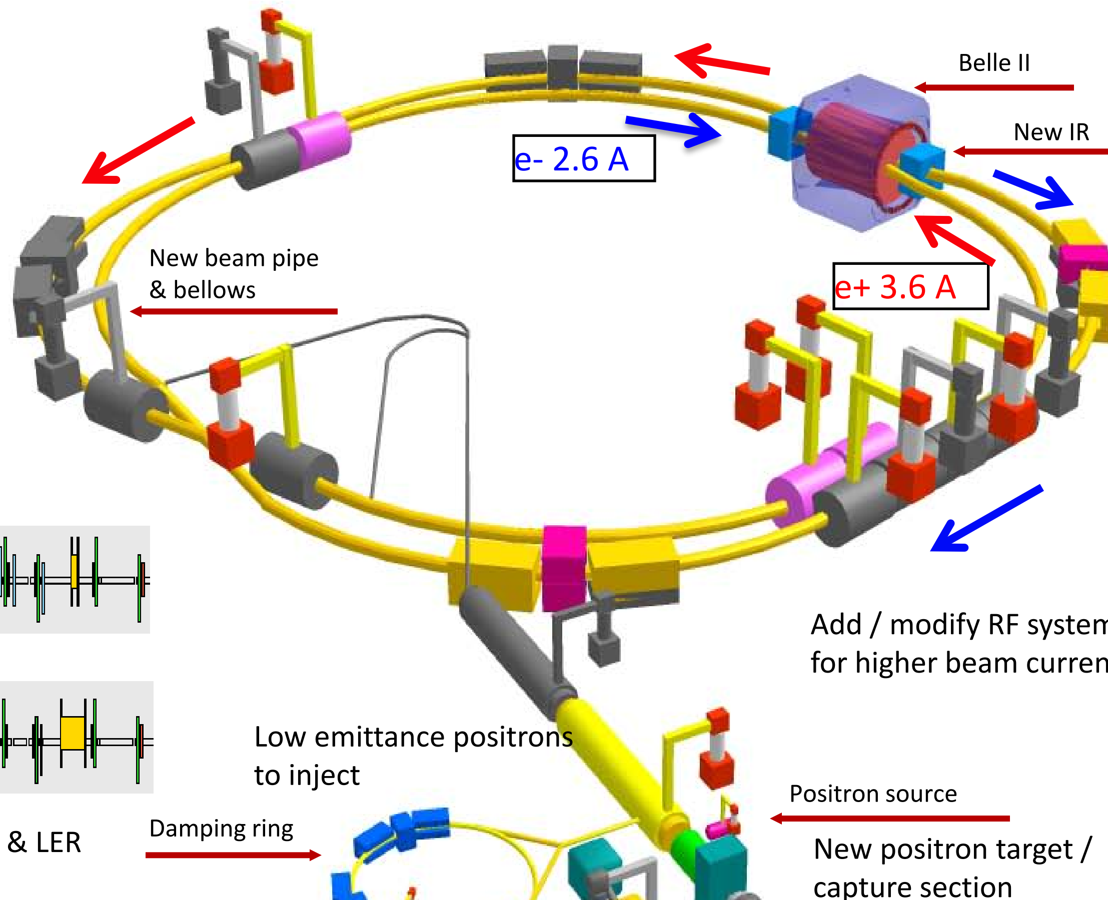

Colliding bunches

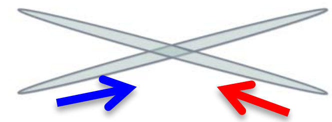

New superconducting /permanent final focusing quads near the IP

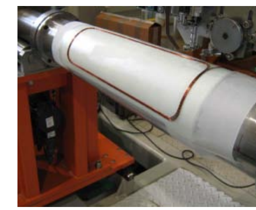

Add / modify RF systems for higher beam current

Low emittance positrons to inject

New positron target / capture section

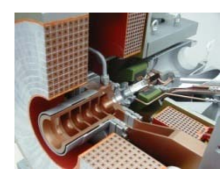

Low emittance electrons to inject

TiN-coated beam pipe with antechambers

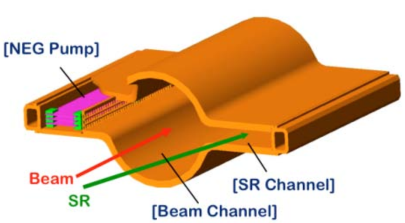

To obtain x40 higher luminosity

2015: Basic hardware (except final focus) now in place

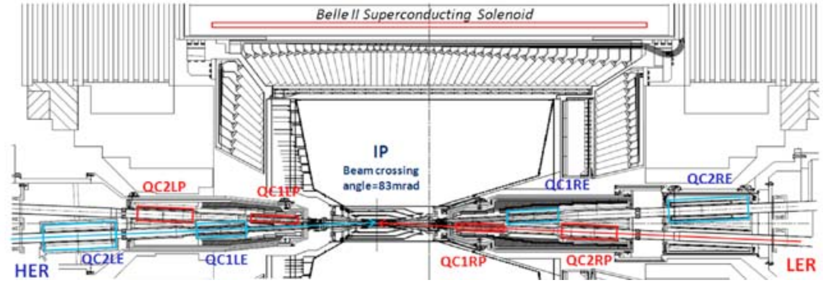

New superconducting final focusing magnets near the IP

e^+ 3.6A

e^- 2.6A

KEKB to SuperKEKB

- Nano-Beam scheme
  - extremely small β_y^*
  - low emittance
- Beam current X 2

$$L = \frac{\gamma_\pm}{2er_e}\left(1+\frac{\sigma_y^*}{\sigma_x^*}\right)\left(\frac{I_\pm \xi_{\pm y}}{\beta_y^*}\right)\left(\frac{R_L}{R_y}\right)$$

40 times higher luminosity
$2.1\text{x}10^{34} \rightarrow 8\text{x}10^{35}$ $cm^{-2}s^{-1}$

Redesign the lattice to reduce the emittance (replace short dipoles with longer ones, increase wiggler cycles) (*all magnets installed 8/2014*)

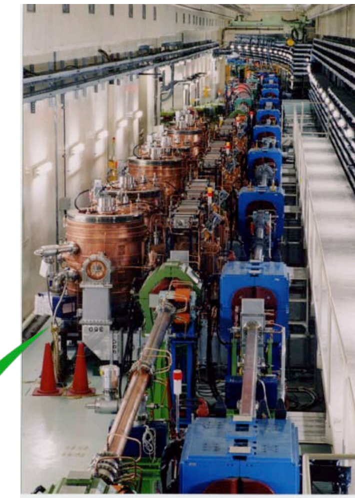

Reinforce RF systems for higher beam currents

Improve monitors and control system

Replace beam pipes with TiN-coated beam pipes with antechambers (*installed*)

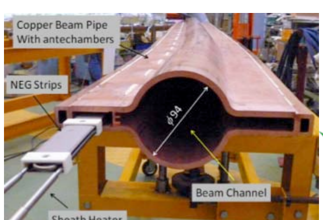

DR tunnel

Injector Linac upgrade

Upgrade positron capture section

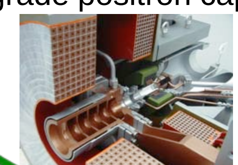

Low emittance RF electron gun

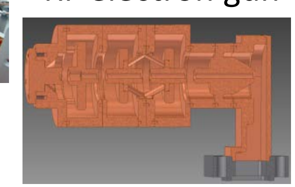

New e+ Damping Ring constructed

Introduction: Measurement principles

R.H. Dicke, Astrophys. Journ., 153, L101, (1968).

- Coded Aperture Imaging:
  - Technique developed by x-ray astronomers using a mask to modulate incoming light. Resulting image must be deconvolved through mask response (including diffraction and spectral width) to reconstruct object.
  - Open aperture of 50% gives high flux throughput for bunch-by-bunch measurements. Heat-sensitive and flux-limiting monochromator not needed.
    - We need such a wide aperture, wide spectrum technique for shot-by-shot (single bunch, single turn) measurements.

E.E. Fenimore and T.M. Cannon, Appl. Optics, V17, No. 3, p. 337 (1978).

- URA (Uniformly Redundant Array) mask
  - Pseudo-random pattern gives relatively flat spatial frequency response.
  - In noiseless, geometric limit, detector image can in principle be inverted directly to give source profile
  - Unfortunately, we don't operate in that limit.
  - Need something like recursive or template fitting.

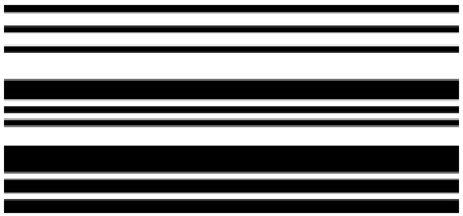

What the detector sees

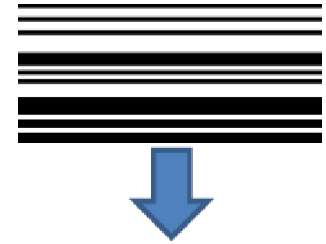

•Source SR wavefront amplitudes:

$$\begin{bmatrix} A_\sigma \\ A_\pi \end{bmatrix} = \frac{\sqrt{3}}{2\pi}\gamma\frac{\omega}{\omega_c}\left(1+X^2\right)(-i)\begin{bmatrix} K_{2/3}(\eta) \\ \frac{iX}{\sqrt{1+X^2}}K_{1/3}(\eta) \end{bmatrix},$$

where

$$X = \gamma\psi,$$

$$\eta = \frac{1}{2}\frac{\omega}{\omega_c}\left(1+X^2\right)^{3/2},$$

K.J. Kim, AIP Conf. Proc. 184 (1989).
J.D. Jackson, "Classical Electrodynamics," (Second Edition),John Wiley & Sons, New York (1975).

•Kirchhoff integral over mask
(+ detector response)
→ Detected pattern:

$$A_{\sigma,\pi}(Detector) = \frac{iA_{\sigma,\pi}(Source)}{\lambda} \times \int_{mask} \frac{t(y_m)}{r_1 r_2} e^{i\frac{2\pi}{\lambda}(r_1+r_2)}\left(\frac{\cos\theta_1+\cos\theta_2}{2}\right)dy_m$$

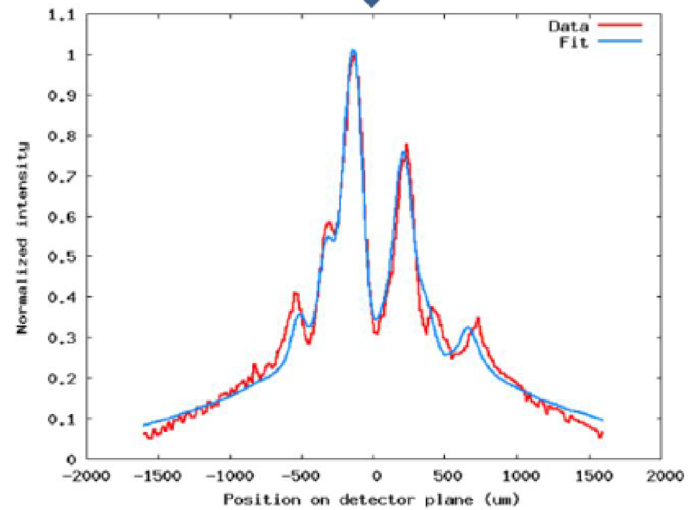

Measured slow-scan detector image (red) at CesrTA, used to validate simulation (blue)

- $t(y_m)$ is complex transmission of mask element at y_m.
- Sum intensities of each polarization and wavelength component.
- Sum weighted set of detector images from point sources.
  - The source beam is considered to be a vertical distribution of point sources.
  - Can also be applied to sources with non-zero angular dispersion and longitudinal extent, for more accurate simulation of emittance and source-depth effects.
  - For machines under consideration here these effects are small, so for computational speed we restrict ourselves to 1-D vertical distributions.

Single-shot resolution estimation

- Want to know, what is chance that a beam of a certain size is misfit as one of a different size?
- Tend to be photon statistics limited. (Thus coded aperture.)
- So:
  - Calculate simulated detector images for beams of different sizes
  - "Fit" images pairwise against each other:
    - One image represents true beam size, one the measured beam size
    - Calculate χ^2/ν residuals differences between images:

N = # pixels/channels
n = # fit parameters (=1, normalization)
S_i = expected number of photons in channel *i*

$$\frac{\chi^2}{\upsilon} = \frac{1}{N-n-1}\sum_{i=1}^{N}\frac{[s_i' - s_i]^2}{\sigma_i^2},$$

    - Weighting function for channel i: $\sigma_i = \sqrt{s_i}\,.$

  - Value of χ^2/ν that corresponds to a confidence interval of 68% is chosen to represent the 1-s confidence interval

Resolution estimates at ATF2

Source of SR: BH3X

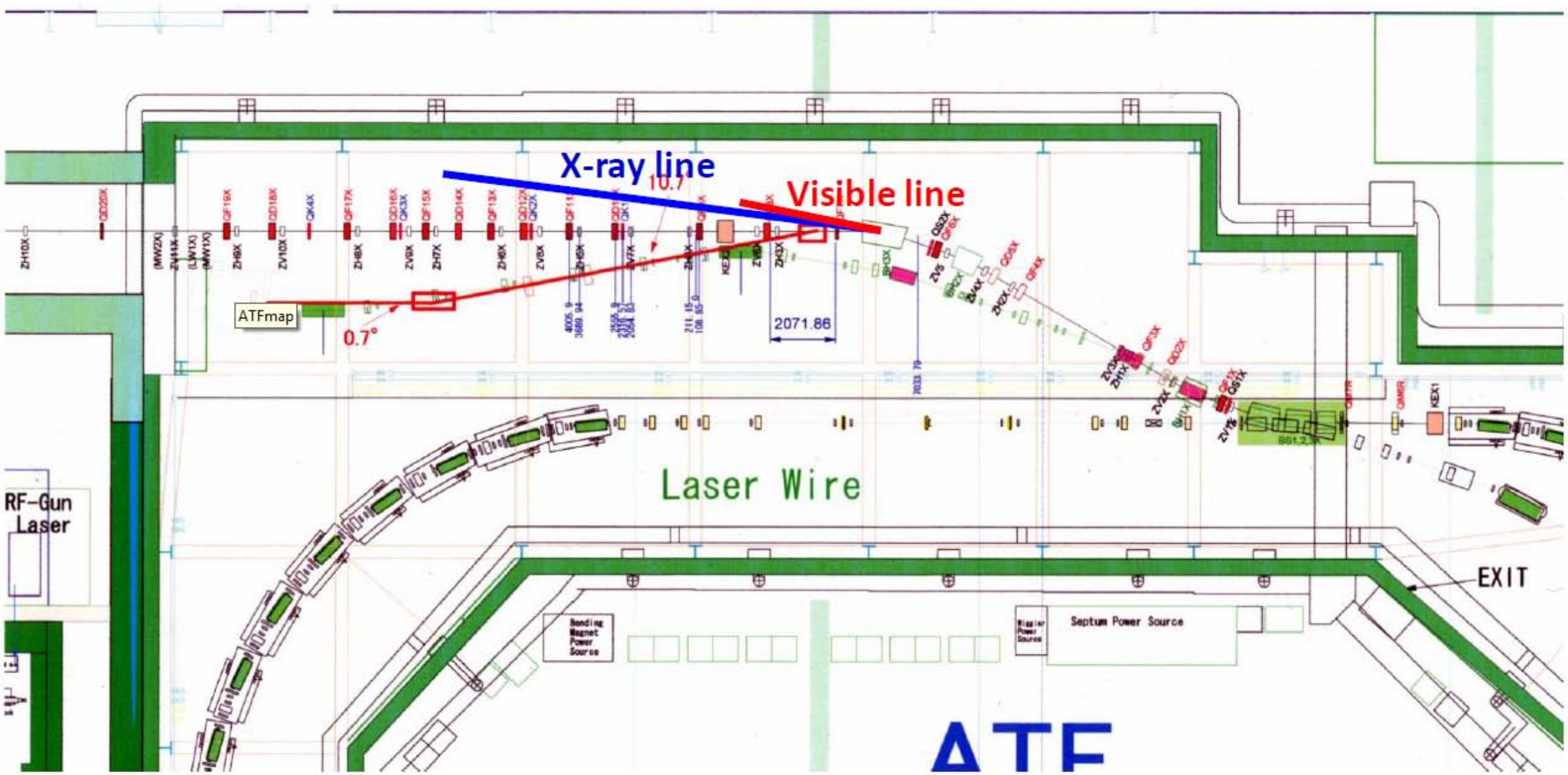

T. Mitsuhashi

ATF2 Beamline

- Extract x-rays from BH3X bend
  - Energy 1.3 Gev, bending radius 4.3 m
  - Critical energy: 1.12 keV
  - 1.5 m from source to CA mask, 9 m from mask to detector
  - Mask:
    - 10 μm 31-element (same as CesrTA)
    - 5 μm 47-element (4 um Ta on ~2 um Ru/SiN/SiC membrane (NTT-AT))
  - Detector: 64-pixel Fermionics InGaAs array
  - Predicted flux at detector: ~250 photons/nC/bunch/50-um pixel

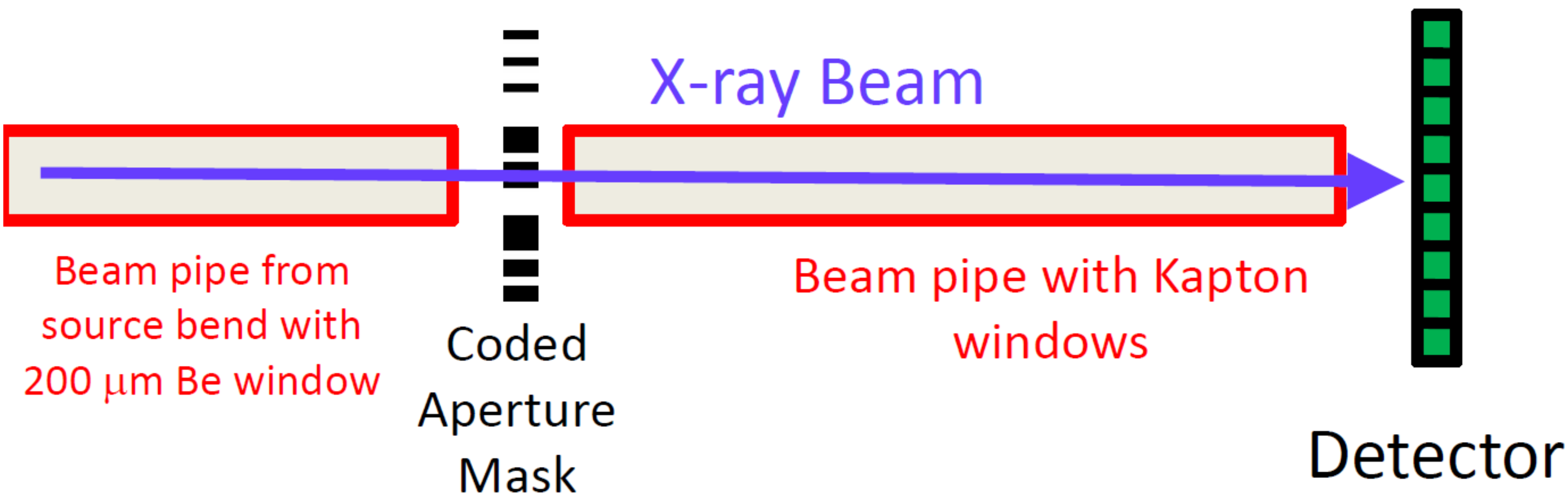

ATF2 x-ray beamline

Under construction

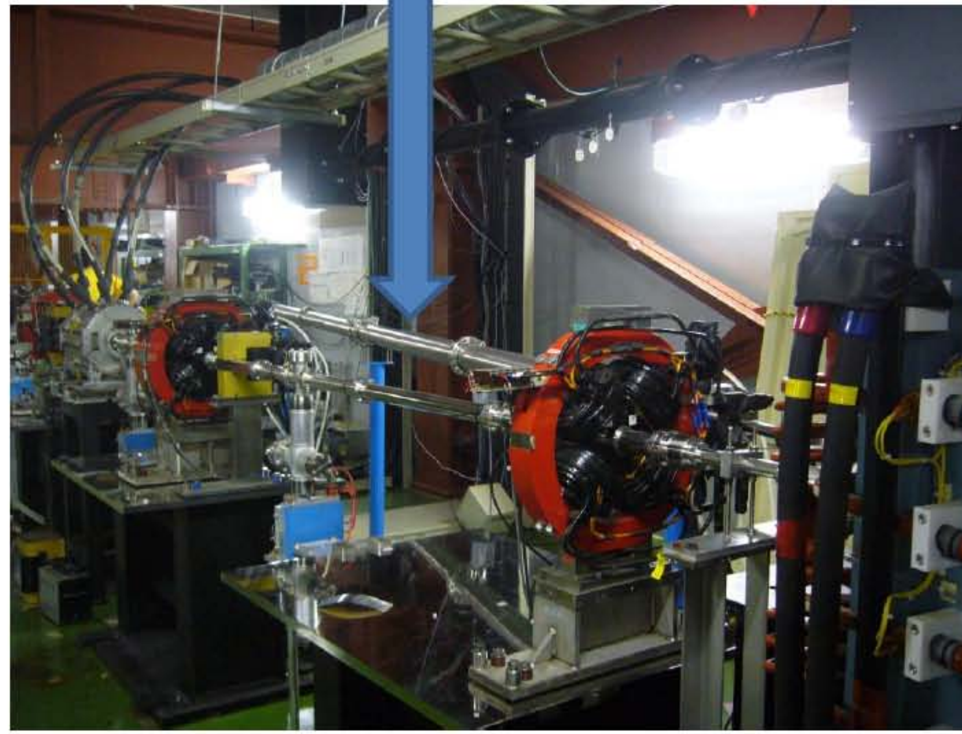

Rotating mask holder

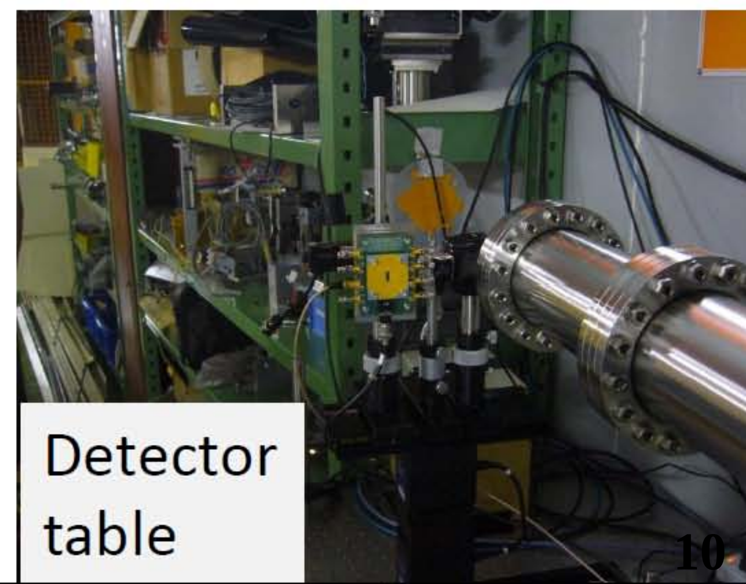

Detector table

47-element, 5 μm/element URA mask @ ATF2

Generate detector images for
various beam sizes:

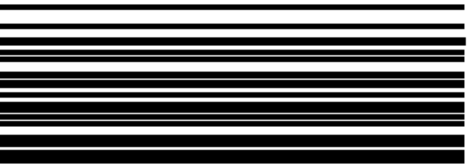

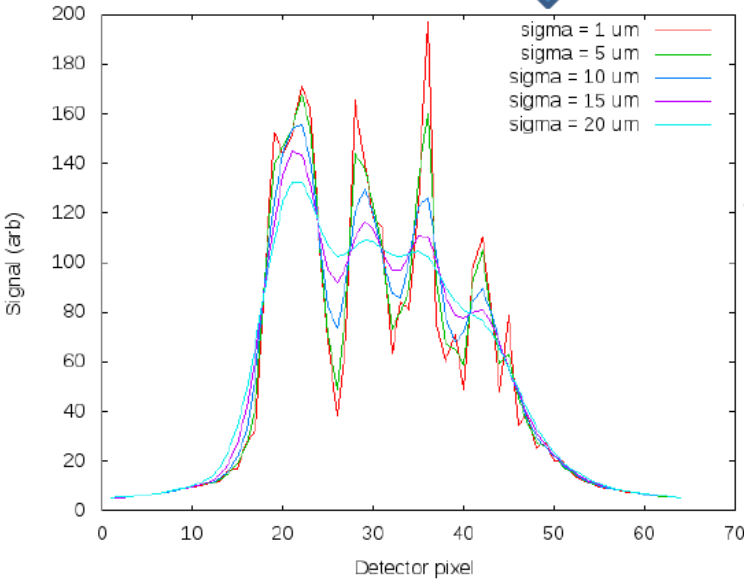

Cross-fit between beam sizes.
Plot 1-sigma statistical confidence regions,
Assuming 200 photons/pixel (average):

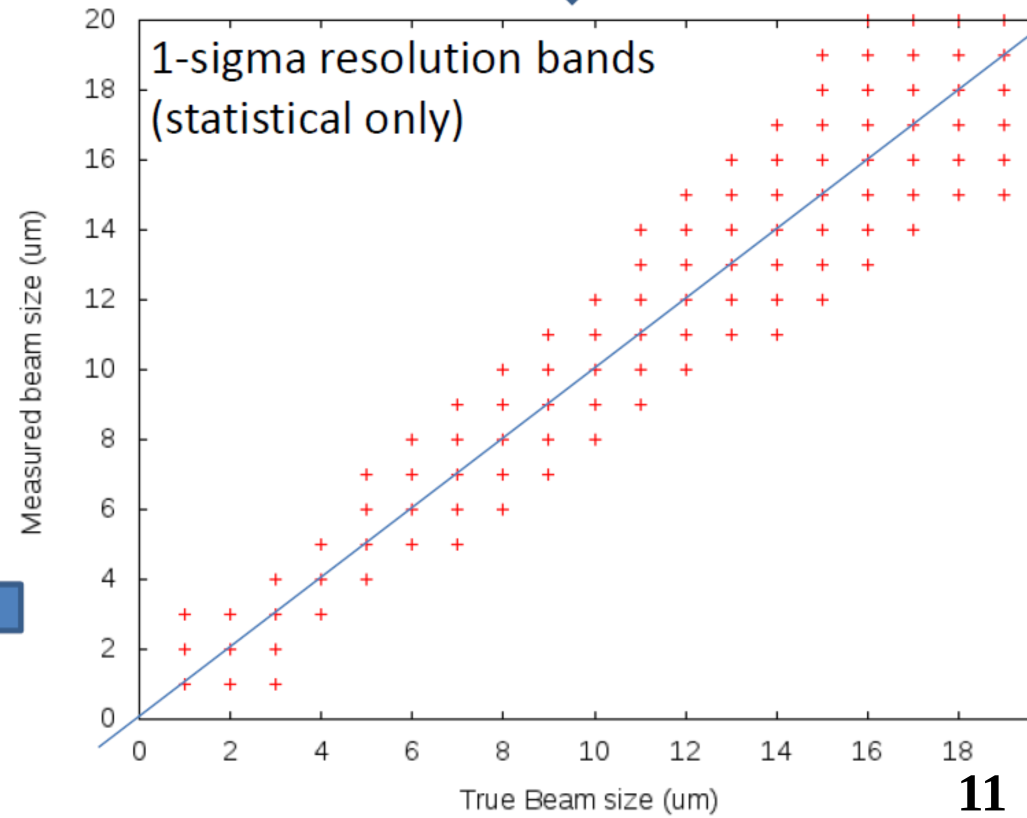

Statistical single-shot
resolution at 4 μm beam size
= +/- ~1 μm
(Assuming ideal detector.)

Resolution estimates: SuperKEKB

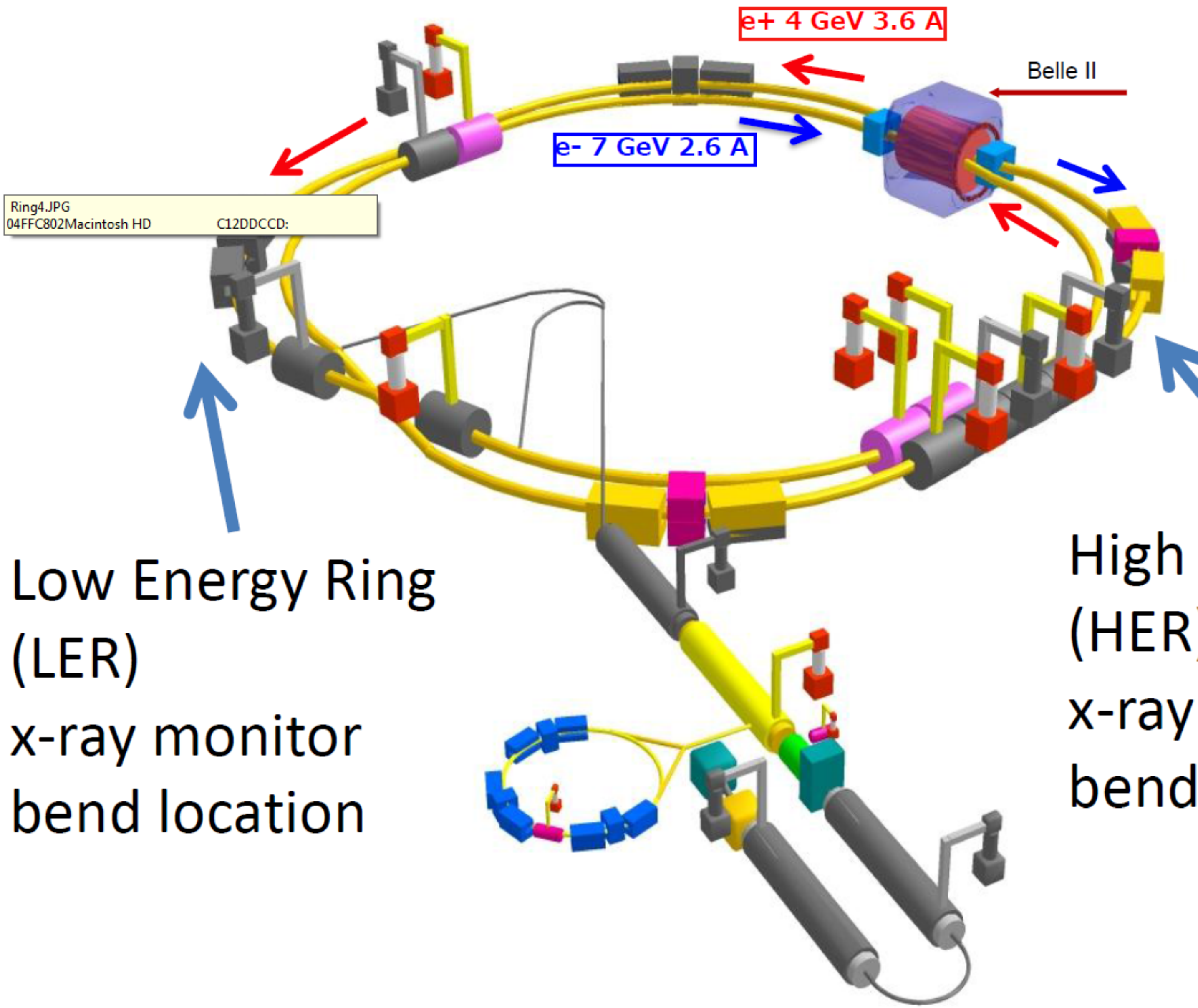

Low Energy Ring (LER) x-ray monitor bend location

High Energy Ring (HER) x-ray monitor bend location

LER X-ray beam line

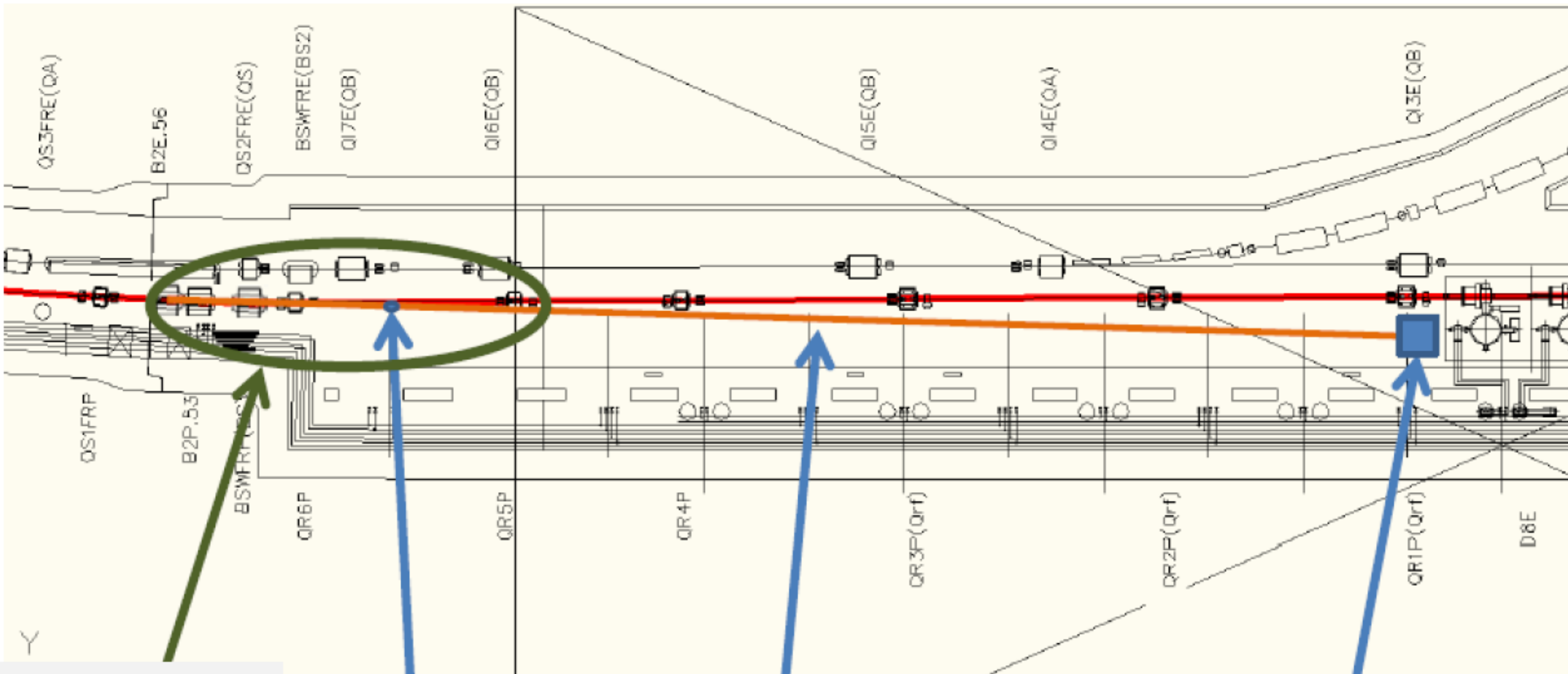

Source and downstream magnets

Optics box

X-ray beam line

Detector Box

SuperKEKB HER X-ray beam

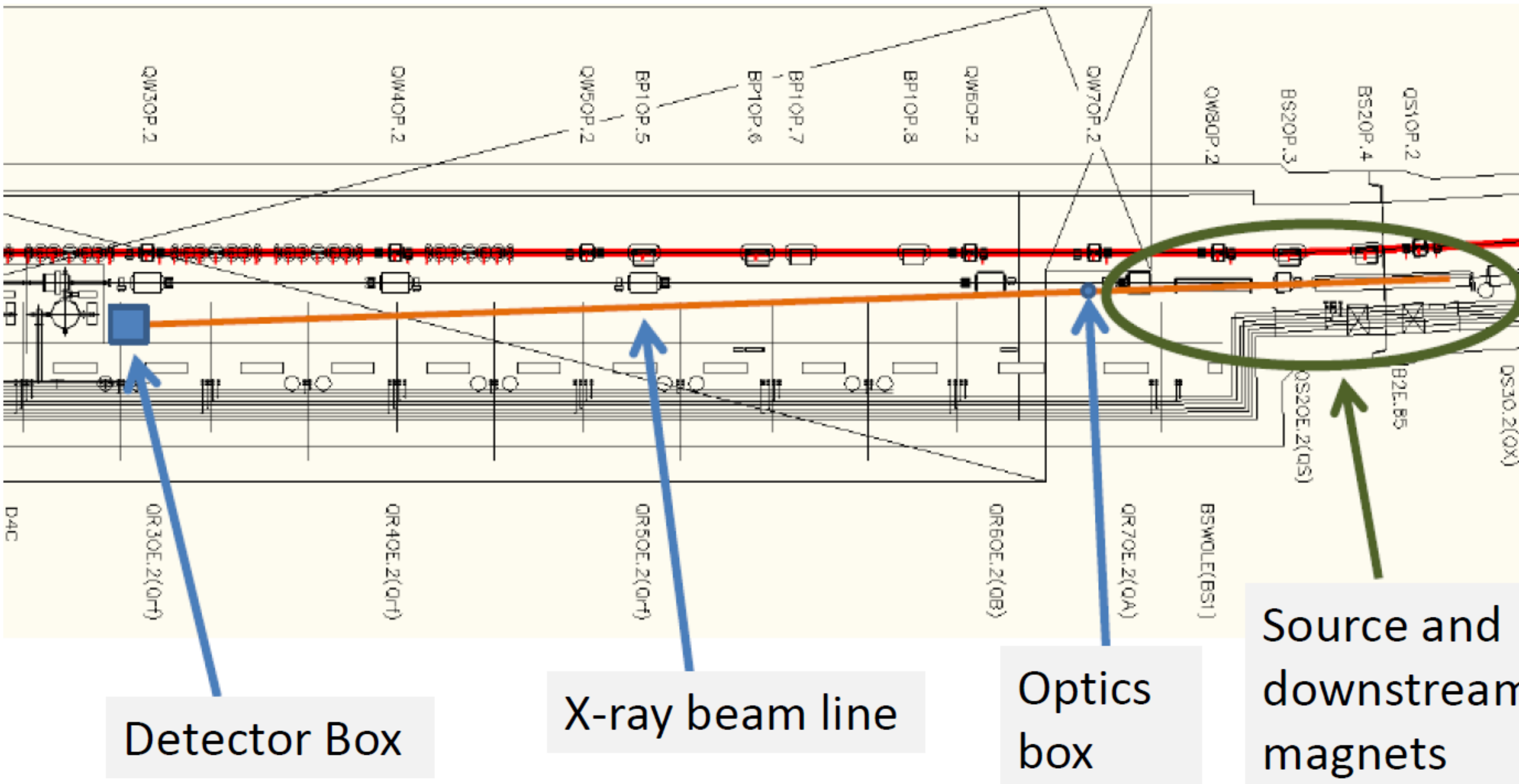

Design Idea

Xray Source Bend Par.	S-LER (BS2FRP.1)	S-HER (BS2E.82)	Units
ε_x	3.20E-09	4.60E-09	m
κ	0.27%	0.24%	
ε_y	8.64E-12	1.10E-11	m
β_y	50.0	11.5	m
σ_y	20.8	11.3	μm
Beam Energy	4	7	GeV
Effective length	0.89	5.9	m
Bend angle	28.0	55.7	mrad
ρ	31.7	105.9	m
Critical Energy	4.4	7.1	keV

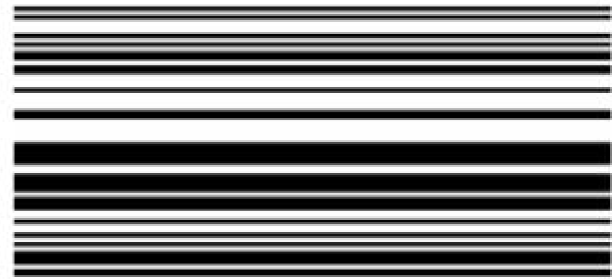

59-element Uniformly Redundant Array mask pattern

Coded Aperture Mask:

- In-hand :
  - High-power, 59-element, 10 μm/element URA
  - 10 μm Au mask on 625 μm Si substrate
- Under development:
  - 20 μm Au mask on 500 μm CVD diamond (monocrystalline) substrate
    - Substrates manufactured.
    - New pattern being designed for improved resolution (E. Mulyani)

Detector:

- 64-pixel (Phase 1), later 128-pixel, 50 μm pitch linear array
- InGaAs detectors in hand (same type as used at CesrTA)
- Deep Si detectors in development for better detection efficiency at high energy (SLAC)

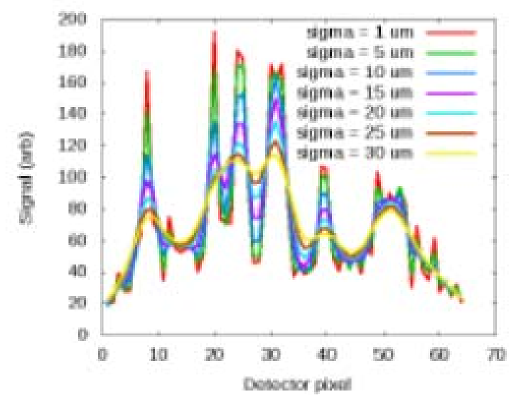

Simulated detector response for various beam sizes at SuperKEKB LER

SuperKEKB Estimated single-shot resolutions (SuperKEKB full current)

- Red points: using 64-pixel detector of same type as at CesrTA
- Green points: using detector with improved photon detection efficiency at higher x-ray energies (not yet developed)

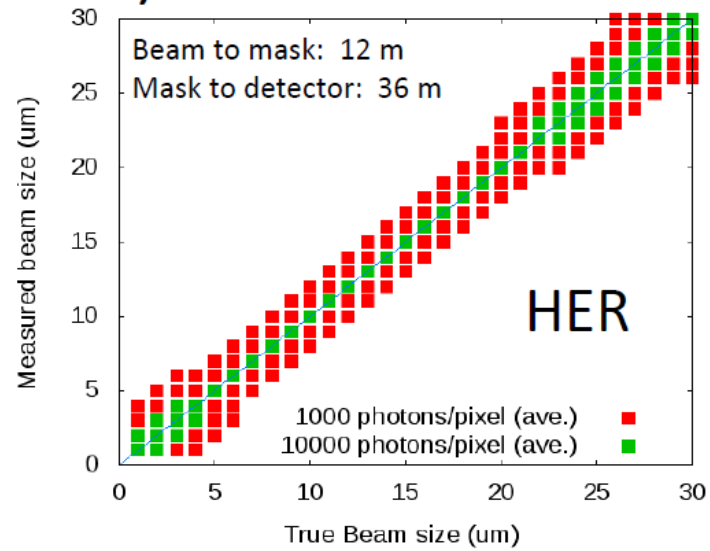

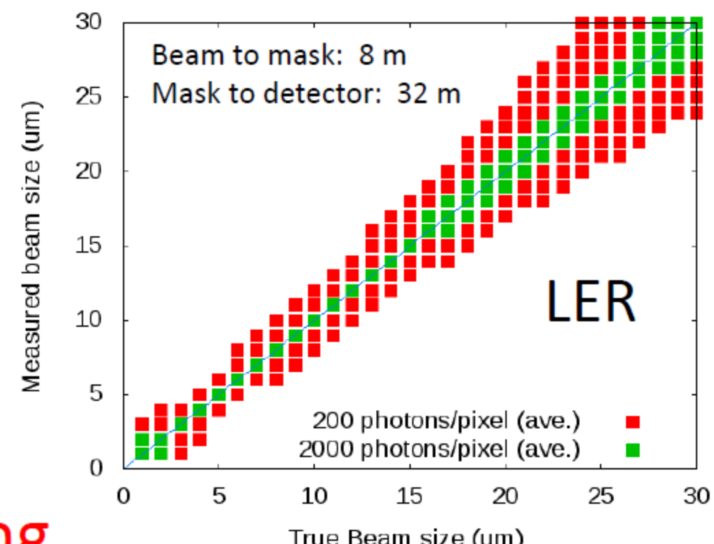

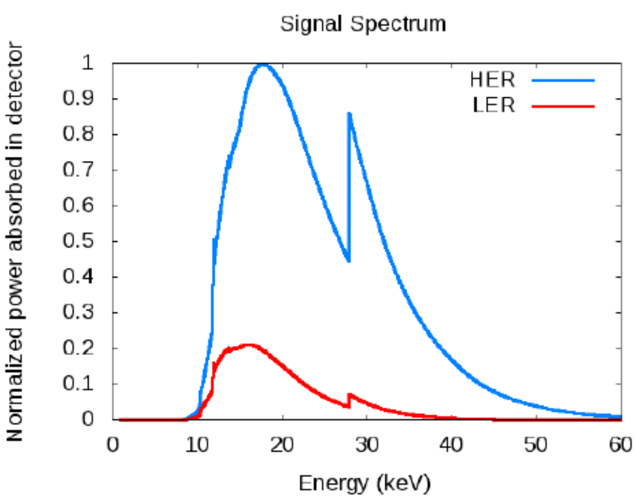

Detected spectrum (Fermionics detector)

Looks promising

Readout basis
IRSX ASIC (PSEC upgrade?)

- Baseline Belle II iTOP ASIC for production

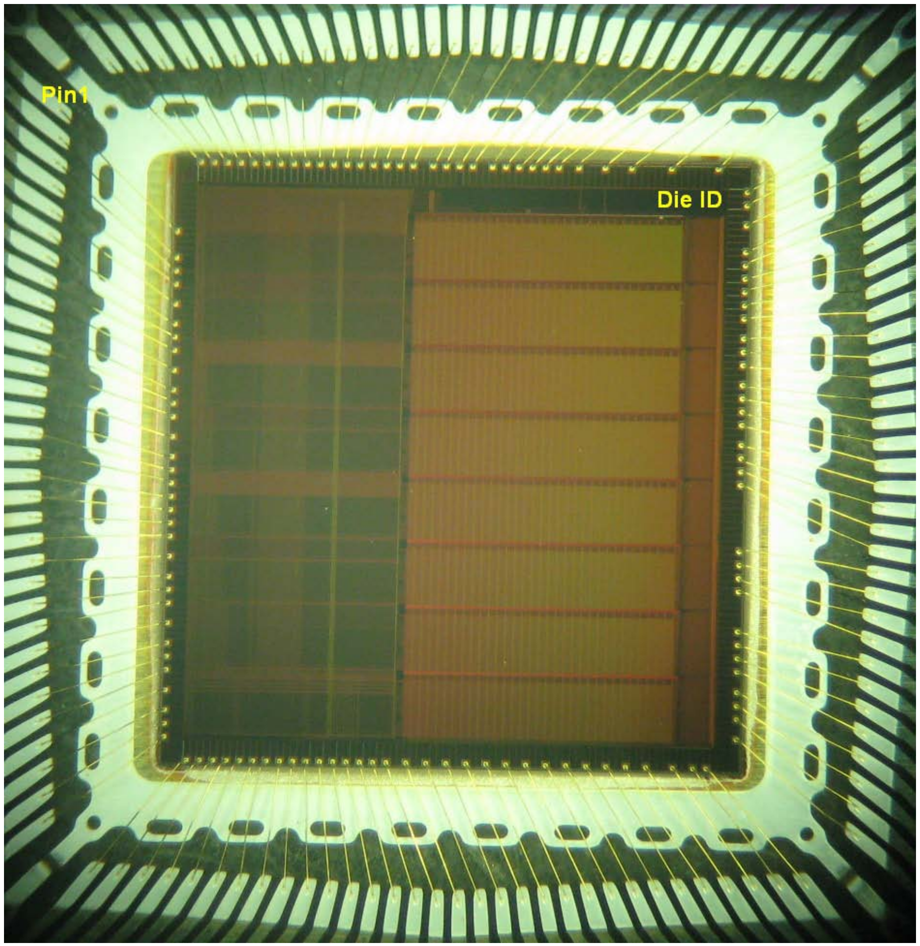

2.6M transistors, 7.7k resistors (DACs)

- High-speed, lower power/EMI LVDS outputs for fast, asynchronous signals
- Extended dynamic range comparator
- Lower-power Gray Code Counter and internal DLL
- High-speed serial readout (many ASICs in parallel)

Interleaved Operation

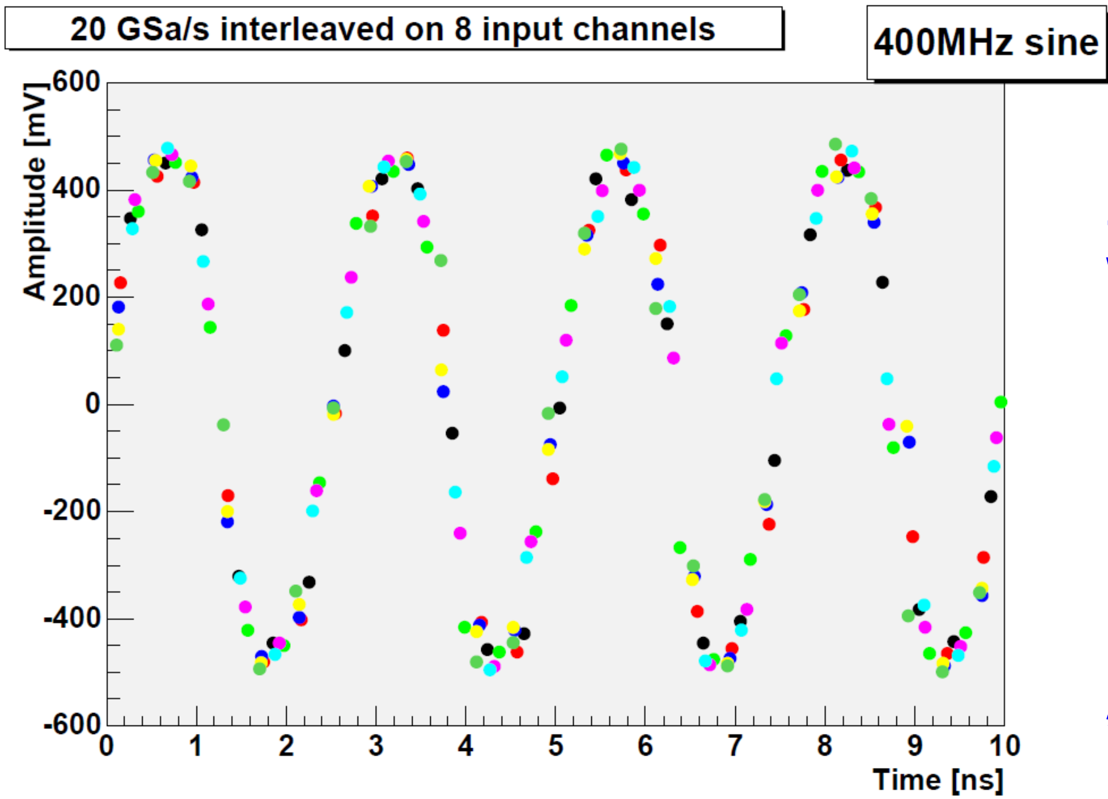

Fig. 23. Example of 20GSa/s interleaved, single-shot waveform recording of a 400MHz sine wave signal on 8 LAB3 input channels, each plotted with a different color.

Demonstrated this back in 2006, but wasn't practical without ability to trim the individual delays (dT's)

Propose to run IRSX in interleave-by-8 mode

10µs orbit / 32,768 samples
~3.3 GSPS
***8 ~ <u>26 GSPS</u>**

The large analog bandwidth recorder and digitizer with ordered readout (LABRADOR) ASIC
G.S. Varner, L.L. Ruckman, (*et al*.), Nucl.Instrum.Meth. **A583** (2007) 447-460.

2015 Initial Install (2x)

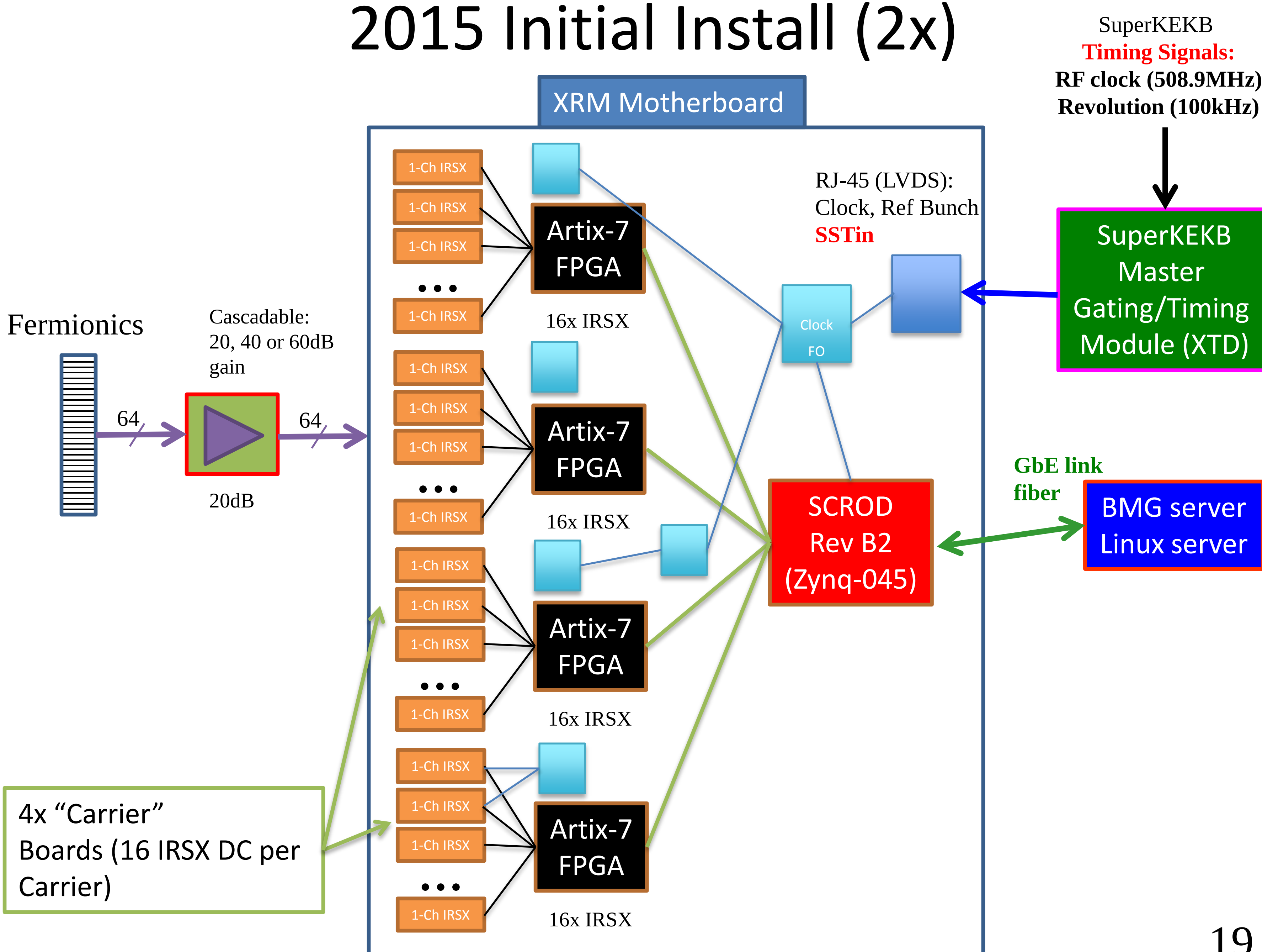

XRM Readout Action Items (besides mechanics)

- **Amplifiers [Vihtori, Peter assist]**
  - ➢ **Are existing, modular 20dB units adequate (noise, stability)**
  - ➢ **Need to verify all channels, or design alternate**
- **Carrier/IRSX DC [Bronson, Gary, Luca]**
  - ➢ **Basic IRSX initialization, configuration**
  - ➢ **Fixed orbit sampling configuration**
  - ➢ **Selectable register data select**
- **SCROD Commissioning [Matt, Luca, James]**
  - ➢ **SCROD – Carrier gigabit communication**
  - ➢ **Variant of the iTOP boardstack control**
  - ➢ **PS data monitoring/distillation**
- **Timing control (XTD) [Khanh, Gary/Peter]**
  - ➢ **From RF 508.8MHz, Revolution, provide timing references**
  - ➢ **Configurable to allow flexible offset (use for other detectors)**

Back-up slides

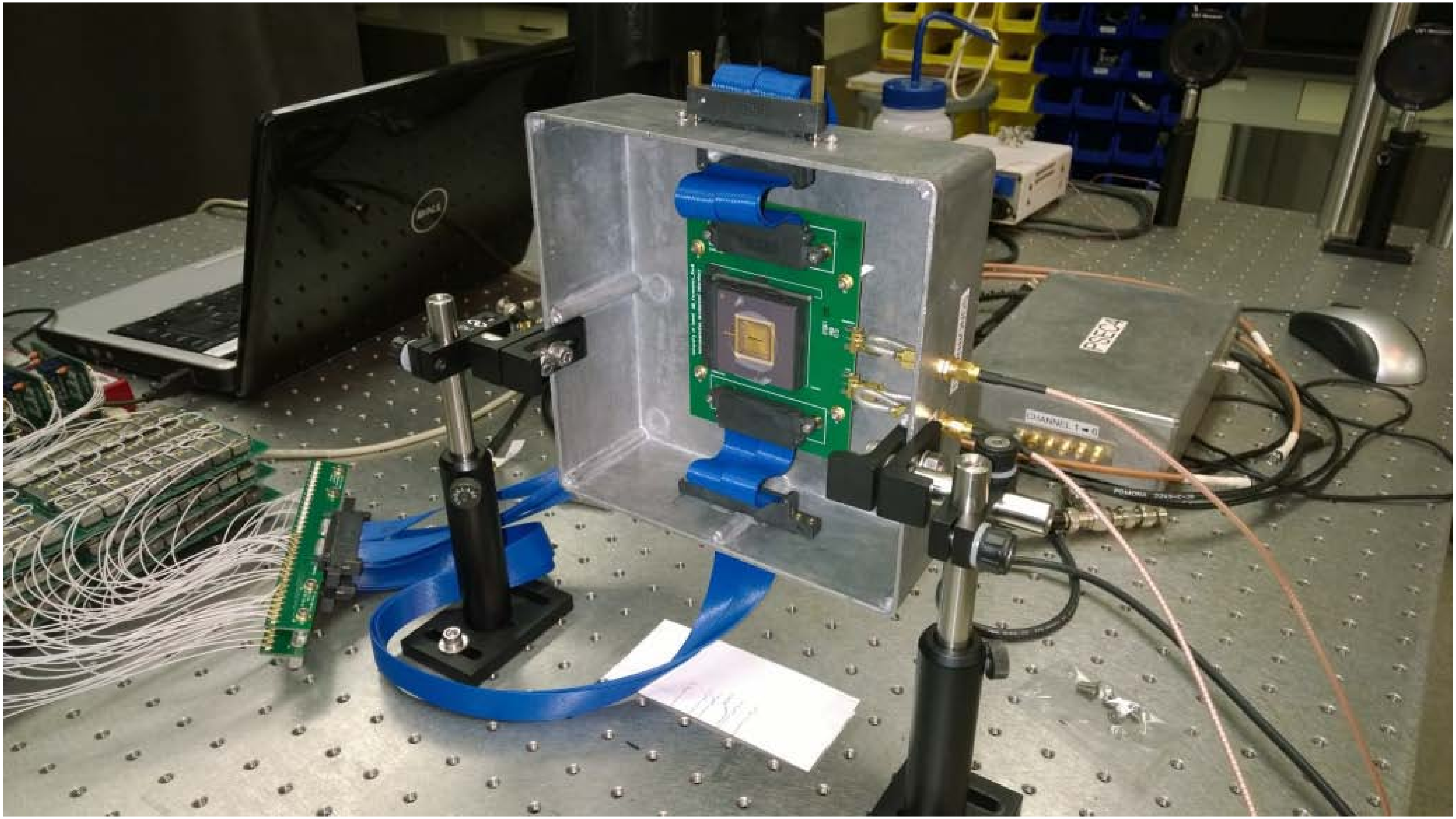

Calibration and Sources of Timing Error

Contributions to timing resolution:

- Voltage uncertainties
- Timing uncertainties

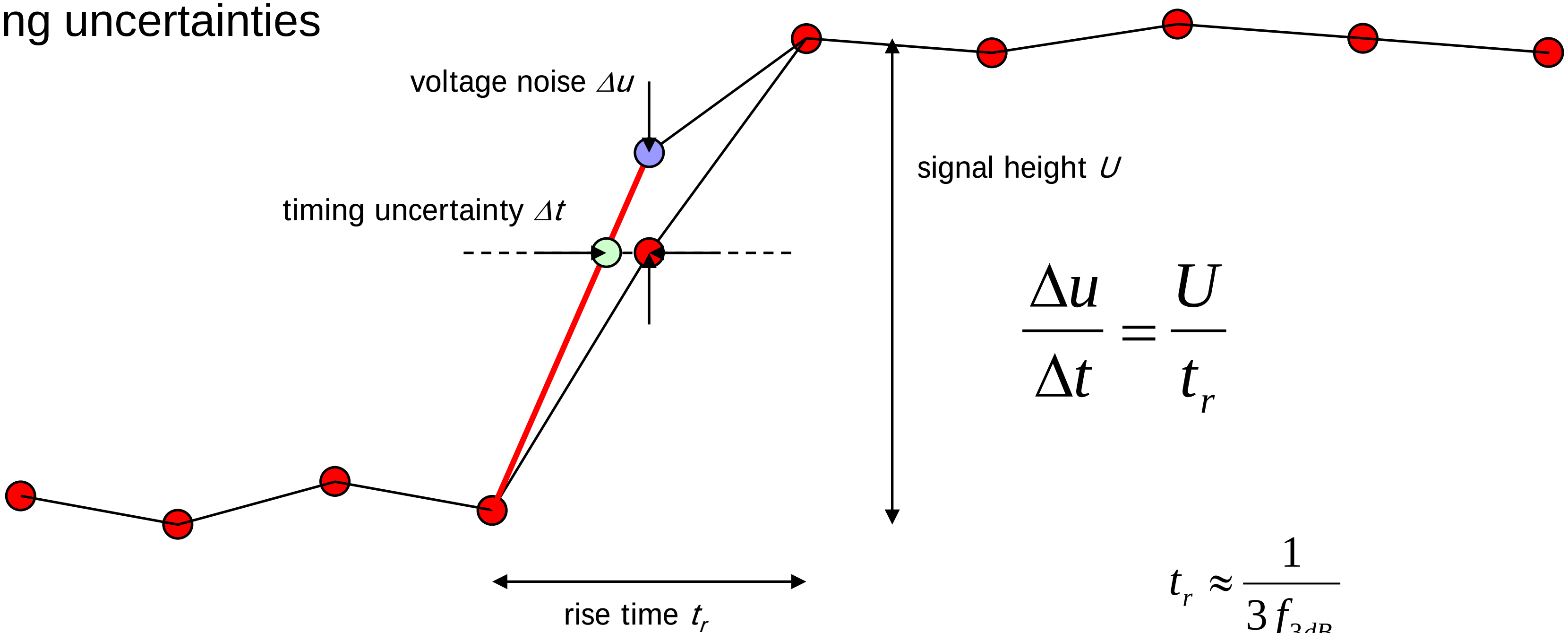

$$\frac{\Delta u}{\Delta t} = \frac{U}{t_r}$$

$$t_r \approx \frac{1}{3 f_{3dB}}$$

$$\Delta t = \frac{\Delta u}{U} \cdot t_r = \frac{\Delta u}{U\sqrt{n}} \cdot t_r = \frac{\Delta u}{U} \cdot \frac{t_r}{\sqrt{t_r \cdot f_s}} = \frac{\Delta u}{U} \cdot \frac{\sqrt{t_r}}{\sqrt{f_s}} = \frac{\Delta u}{U} \cdot \frac{1}{\sqrt{3 f_s \cdot f_{3dB}}}$$

*Diagram, formulas from Stefan Ritt

Calibration and Sources of Timing Error

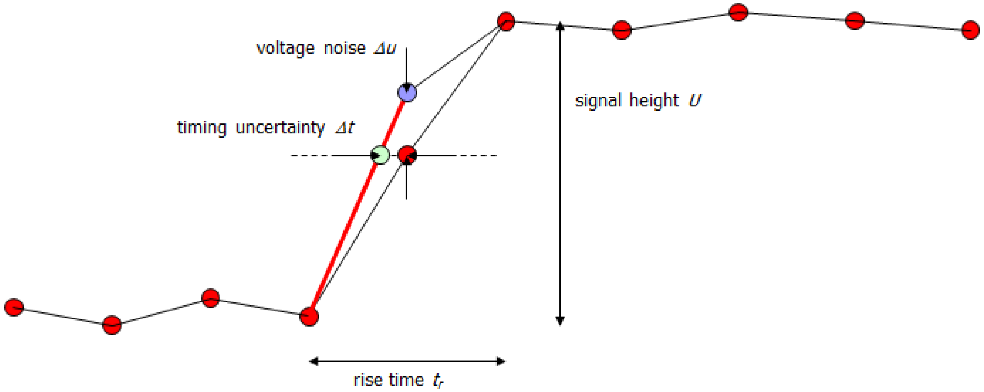

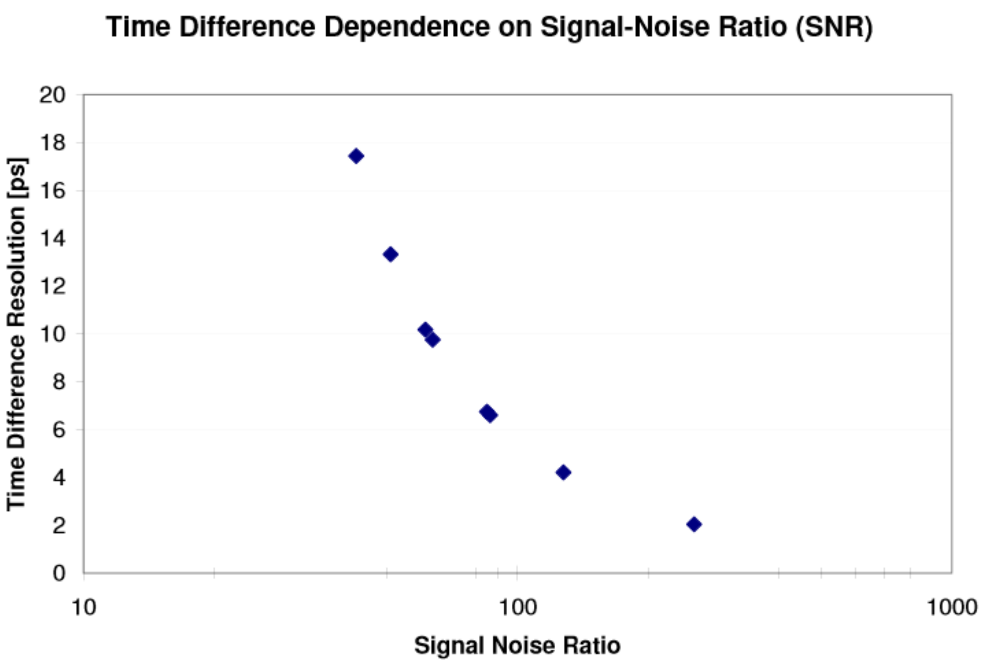

$\Delta u = 2\mathrm{mV}$
$U = 1\mathrm{V}$
$f_s = 26$ GSPS
$f_{3dB} = 1.2\mathrm{GHz}$

$$\frac{\Delta u}{U} \cdot \frac{1}{\sqrt{3 f_s \cdot f_{3dB}}} \sim 200 \text{ fs}$$

Aperture stability is key

Timing Uncertainties and Timing Calibration

- Time interval between delay line stages has intrinsic variation.
- Not accounting for this properly causes significant timing error

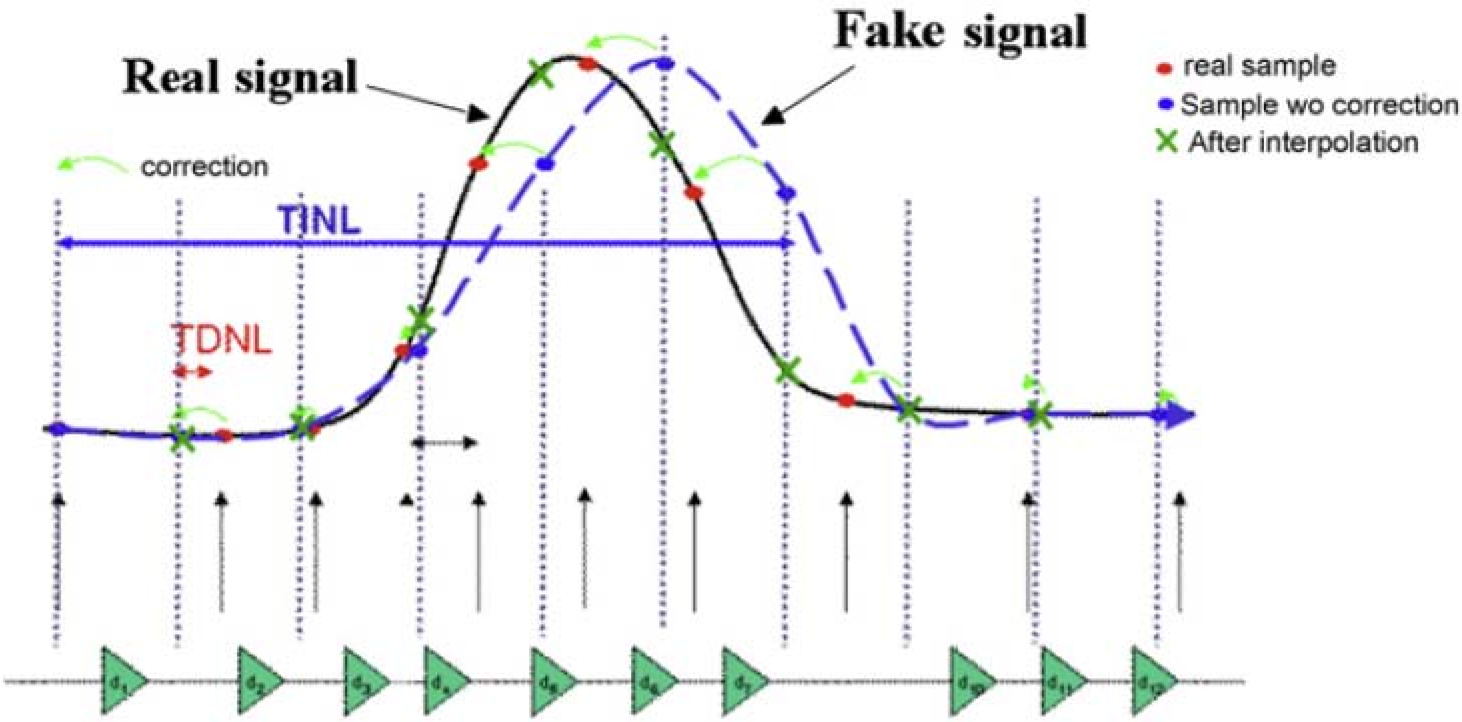

Nuclear Instruments and Methods in Physics Research A 629 (2011) 123–132

Result: visually nicer waveforms

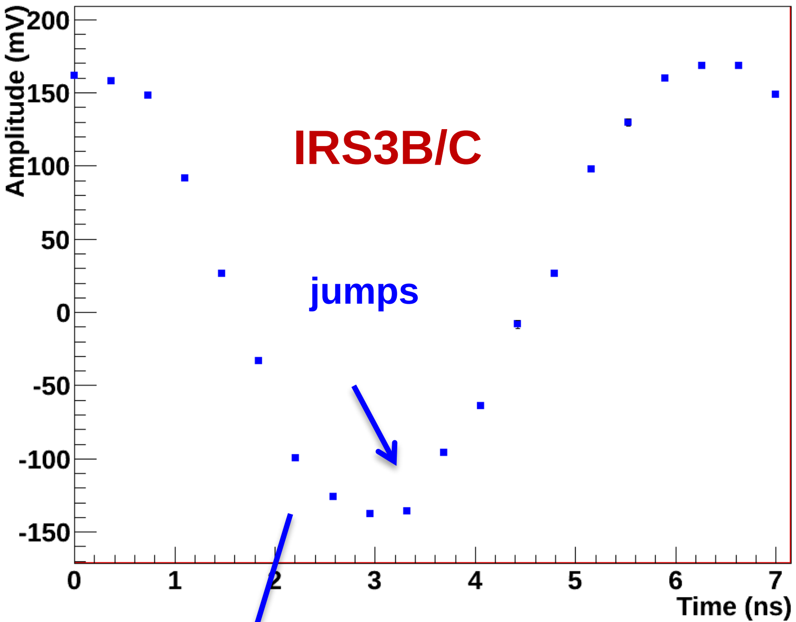

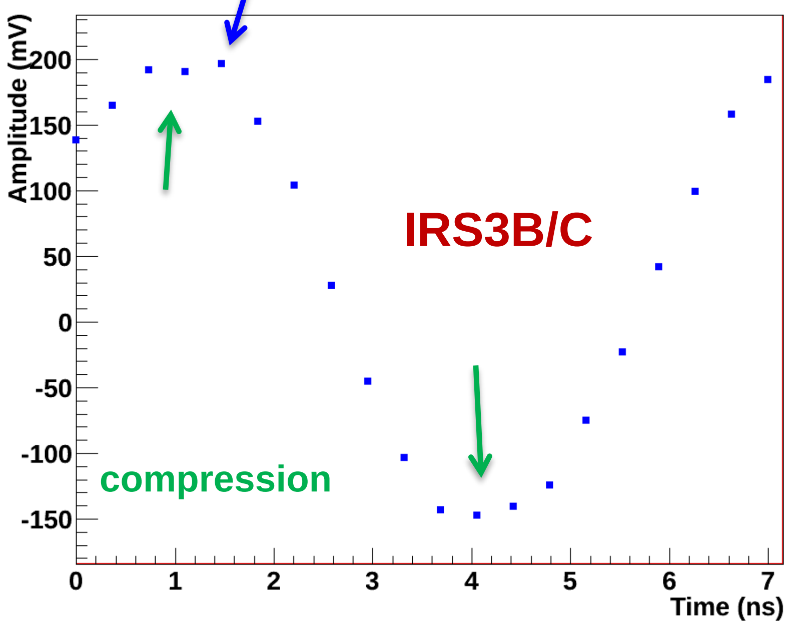

Difference most evident at the extrema of the waveforms

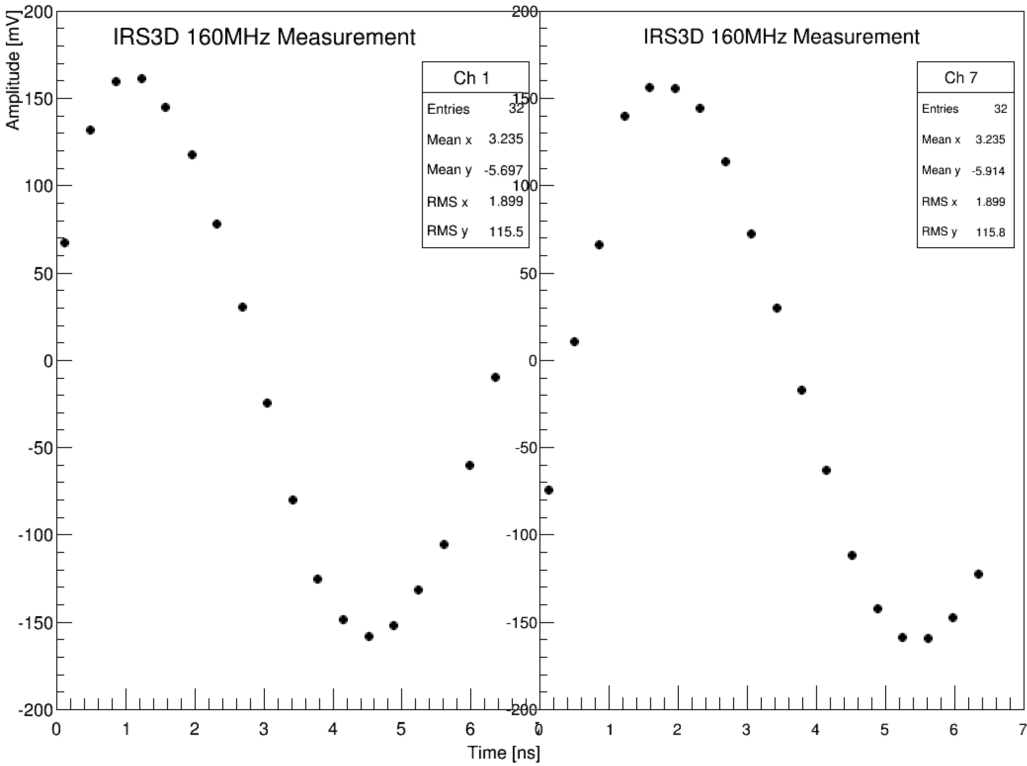

IRS3D

Time base non-uniformity…

2.6 GSa/s

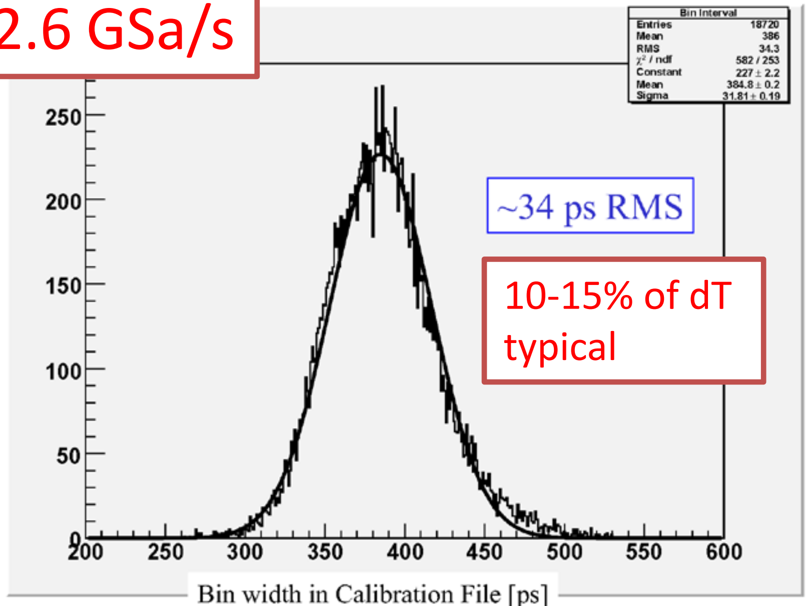

~34 ps RMS

10-15% of dT typical

If can correct, reduces processing time dramatically, as this is the most computationally-intensive aspect of "fast feature extraction"

Revised Full System Overview